J|A|C|S
ARTICLES
Published on Web 06/05/2004

Determinants of the Relative Reduction Potentials of Type-1 Copper Sites in Proteins

Hui Li,[†] Simon P. Webb,[‡] Joseph Ivanic,[‡] and Jan H. Jensen*,[†]

Contribution from the Department of Chemistry, The University of Iowa, Iowa City, Iowa 52242, and Advanced Biomedical Computing Center, SAIC-Frederick, National Cancer Institute at Frederick, P.O. Box B, Frederick, Maryland 21702

Received February 5, 2004; E-mail: Jan-Jensen@uiowa.edu

Abstract: The relative Cu^{2+}/Cu^{+} reduction potentials of six type-1 copper sites (cucumber stellacyanin, *P. aeruginosa* azurin, poplar plastocyanin, *C. cinereus* laccase, *T. ferrooxidans* rusticyanin, and human ceruloplasmin), which lie in a reduction potential range from 260 mV to over 1000 mV, have been studied by quantum mechanical calculations. The range and relative orderings of the reduction potentials are reproduced very well compared to experimental values. The study suggests that the main structural determinants of the relative reduction potentials of the blue copper sites are located within 6 Å of the Cu atoms. Further analysis suggests that the reduction potential differences of type-1 copper sites are caused by axial ligand interactions, hydrogen bonding to the S_{Cys}, and protein constraint on the inner sphere ligand orientations. The low reduction potential of cucumber stellacyanin is due mainly to a glutamine ligand at the axial position, rather than a methionine or a hydrophobic residue as in the other proteins. A stronger interaction with a backbone carbonyl group is a prime contributor to the lower reduction potential of *P. aeruginosa* azurin as compared to poplar plastocyanin, whereas the reverse is true for *C. cinereus* laccase and *T. ferrooxidans* rusticyanin. The lack of an axial methonine ligand also contributes significantly to the increased reduction potentials of *C. cinereus* laccase and human ceruloplasmin. However, in the case of *C. cinereus* laccase, this increase is attenuated by the presence of only one amide NH hydrogen bond to the S_{Cys} rather than two in the other proteins. In human ceruloplasmin the reduction potential is further increased by the structural distortion of the equatorial ligand orientation.

I. Introduction

Electron-transfer reactions integrate the respiratory and anabolic/catabolic pathways in living cells. Metalloredox proteins, i.e., electron-transfer proteins and oxido-reductase enzymes, play central roles in these reactions because of their suitable reduction potentials and fast electron-transfer rates.[1] Understanding the molecular determinants of these redox properties will aid significantly in designing new redox active proteins and enzymes.[2−4] The most studied metalloredox proteins include Fe−S proteins, hemoproteins, copper proteins, and molybdoenzymes.[1] In this work, the relative reduction potentials of blue copper proteins[5,6] (BCPs) and blue multicopper oxidases[5,7] that contain type-1 (T1) copper centers are studied.

A T1 copper center has at least three coordination ligands: one cysteine residue and two histidine residues. The unusual strong blue color (∼600 nm) and small paramagnetic hyperfine coupling constant ($A_{||}$) of the oxidized form arise solely from the short (<2.3 Å) and highly covalent $Cu^{2+}-S_{Cys}$ bond.[8−11] There is usually a fourth, axial, ligation provided by a methionine or glutamine side chain. Additional (fifth) ligation is occasionally provided by a carbonyl group from the protein backbone. T1 sites exhibit very little geometrical change upon reduction as shown by X-ray crystal structures, leading to high electron-transfer rates. The Cu^{2+}/Cu^{+} reduction potentials of T1 copper centers vary considerably from 184 mV (Japanese lacquer tree or *Rhus vernicifera* stellacyanin[12]) to 680 mV (*T. ferrooxidans* rusticyanin[5,6]) and to above 1000 mV (human ceruloplasmin[13]). The reduction potentials are generally much higher than that of the aqueous Cu^{2+}/Cu^{+} pair (154 mV) and inorganic copper complexes. Type-2 and type-3 copper centers,

[†] Department of Chemistry, The University of Iowa.
[‡] Advanced Biomedical Computing Center, SAIC-Frederick, National Cancer Institute at Frederick.

(1) Cowan, J. A. *Inorganic Biochemistry: An Introduction*; VCH Publishers: New York, 1993.
(2) Barker, P. D. *Curr. Opin. Struct. Biol.* **2003**, *13*, 490−499.
(3) Gilardi, G.; Fantuzzi, A.; Sadeghi, S. J. *Curr. Opin. Struct. Biol.* **2001**, *11*, 491−499.
(4) Kennedy, M. L.; Gibney, B. R. *Curr. Opin. Struct. Biol.* **2001**, *11*, 485−490.
(5) Lappin, A. G. In *Metal Ions in Biological Systems*; Sigel, H., Ed.; Marcel Dekker: New York, 1981; Vol. 13, pp 15−72.
(6) Sykes, A. G. In *Advances in Inorganic Chemistry*; Sykes, A. G., Ed.; Academic Press: San Diego, 1991; Vol. 36, pp 377−408.
(7) Urbach, F. L. In *Metal Ions in Biological Systems*; Sigel, H., Ed.; Marcel Dekker: New York, 1981; Vol. 13, pp 73−116.
(8) Ryde, U.; Olsson, M. H. M.; Roos, B. O.; Borin, A. C. *Theor. Chem. Acc.* **2001**, *105*, 452−462.
(9) Pierloot, K.; DeKerpel, J. O. A.; Ryde, U.; Roos, B. O. *J. Am. Chem. Soc.* **1997**, *119*, 218−226.
(10) Canters, G. W.; Gilardi, G. *Febs Lett.* **1993**, *325*, 39−48.
(11) Mizoguchi, T. J.; Dibilio, A. J.; Gray, H. B.; Richards, J. H. *J. Am. Chem. Soc.* **1992**, *114*, 10 076−10 078.
(12) Sailasuta, N.; Anson, F. C.; Gray, H. B. *J. Am. Chem. Soc.* **1979**, *101*, 455−458.
(13) Machonkin, T. E.; Zhang, H. H.; Hedman, B.; Hodgson, K. O.; Solomon, E. I. *Biochemistry* **1998**, *37*, 9570−9578.

10.1021/ja049345y CCC: $27.50

Fe−S, heme and other redox centers also show a variety of reduction potential values in different protein environments.[1] The general molecular determinants of the reduction potential variations are of considerable interest. On the basis of decades of work on metalloredox proteins, five main determinants have been proposed:

(1) Desolvation (aka hydrophobic) effects; for example, a hydrophobic environment raises the Cu^{2+}/Cu^{+} reduction potential by a net preferential stabilization of the less charged Cu^{+} oxidation state. X-ray and NMR determined structures show that all T1 copper sites are embedded in a highly hydrophobic region of nonpolar side chains, which may account for their generally high reduction potentials.[14−18] The very high reduction potential of *T. ferrooxidans* rusticyanin (680 mV) has been attributed to its unusually high hydrophobicity,[14,15,18,19] compared to those of other blue copper proteins. However, a quantitative relationship between the hydrophobicity and reduction potential is difficult to establish experimentally.

(2) Metal−ligand interactions; for example, replacing the copper ligand Gln99 by a nonligating Leu increases the reduction potential of cucumber stellacyanin by 320 mV.[20] In general, site-directed mutagenesis studies of T1 copper sites show that the axial ligands (methionine, glutamine, and glutamate) can stabilize the Cu^{2+} to different extents, thus decreasing the reduction potentials by different amounts (100∼400 mV).[20−29] However, some T1 sites that have the same axial ligation (e.g., same axial Met group in *P. aeruginosa* azurin, poplar plastocyanin, and *T. ferrooxidans* rusticyanin) or have no axial ligation (e.g., some fungal laccases[30,31]) still show a considerable range (∼350 mV) of reduction potentials. Thus, it is clear that axial ligand interactions cannot be the sole determinant of the observed reduction potential range of 184−1000 mV in T1 copper sites.

(3) Hydrogen bonding to metal bound S atoms;[17,32−37] for example, one more backbone hydrogen bond to the copper bound S_{Cys} in Pro80Ala and Pro80Ile mutants of *A. faecalis* pseudoazurin results in higher reduction potentials (increased by 139 and 180 mV, respectively)[35] due to the net destabilization of the Cu^{2+} oxidation state. This general effect can be captured by purely electrostatic models,[38] suggesting that the net destabilization may simply be a result of the electrostatic repulsion between the N−H dipole and Cu^{2+}. Similar effects are shown in Fe−S proteins by backbone engineering studies.[34]

(4) Protein constraint (aka entatic/rack mechanism); for example, the protein fold can modulate the T1 copper reduction potential by dictating the positions and orientations of the Cu ligands and adjusting the coordination bond strengths.[20,36,39−41] Protein constraint has been used to explain the reduction potential change of *P. aeruginosa* azurin on going from the folded state (320 mV) to the partially unfolded high-potential-state (420 mV) and to the unfolded state (460 mV).[39,41] Unfortunately, no quantitative relationship between constraints and reduction potential has been established. Some theoretical studies have argued that the protein imposes relatively little strain on T1 copper sites.[42,43]

(5) Intraprotein electrostatic (aka charge−charge and dipole-charge) interactions;[21,22,26,27,29,37,42,44−47] for example, replacing Met44 by a Lys in *P. aeruginosa* azurin increases the reduction potential by 40∼60 mV,[44] due to the net destabilization of the Cu^{2+} oxidation state caused by the repulsion between the Lys^{+} and Cu^{2+}. In general, site-directed mutations with charged groups typically change reduction potentials by ∼50 mV.[21,22,26,27,29,37,44−46] Dipole interactions from the protein peptide backbone and the polar side chain groups may be more important according to some theoretical studies.[42,47]

Computational methods for prediction of metalloprotein reduction potentials are usually based on classical electrostatic calculations[48−50] and use either continuum electrostatics[51−54] or

(14) Walter, R. L.; Ealick, S. E.; Friedman, A. M.; Blake, R. C.; Proctor, P.; Shoham, M. *J. Mol. Biol.* **1996**, *263*, 730−751.
(15) Kyritsis, P.; Dennison, C.; Ingledew, W. J.; McFarlane, W.; Sykes, A. G. *Inorg. Chem.* **1995**, *34*, 5370−5374.
(16) Donaire, A.; Jimenez, B.; Moratal, J. M.; Hall, J. F.; Hasnain, S. S. *Biochemistry* **2001**, *40*, 837−846.
(17) Donaire, A.; Jimenez, B.; Fernandez, C. O.; Pierattelli, R.; Niizeki, T.; Moratal, J. M.; Hall, J. F.; Kohzuma, T.; Hasnain, S. S.; Vila, A. J. *J. Am. Chem. Soc.* **2002**, *124*, 13 698−13 708.
(18) Jimenez, B.; Piccioli, M.; Moratal, J. M.; Donaire, A. *Biochemistry* **2003**, *42*, 10 396−10 405.
(19) Jimenez, B.; Donaire, A.; Moratal, J. M.; Piccioli, M.; Hall, J. F.; Hasnain, S. S. *J. Inorg. Biochem.* **2001**, *86*, 282−282.
(20) George, S. D.; Basumallick, L.; Szilagyi, R. K.; Randall, D. W.; Hill, M. G.; Nersissian, A. M.; Valentine, J. S.; Hedman, B.; Hodgson, K. O.; Solomon, E. I. *J. Am. Chem. Soc.* **2003**, *125*, 11 314−11 328.
(21) Karlsson, B. G.; Tsai, L. C.; Nar, H.; SandersLoehr, J.; Bonander, N.; Langer, V.; Sjolin, L. *Biochemistry* **1997**, *36*, 4089−4095.
(22) Hall, J. F.; Kanbi, L. D.; Strange, R. W.; Hasnain, S. S. *Biochemistry* **1999**, *38*, 12 675−12 680.
(23) Xu, F.; Berka, R. M.; Wahleithner, J. A.; Nelson, B. A.; Shuster, J. R.; Brown, S. H.; Palmer, A. E.; Solomon, E. I. *Biochem. J.* **1998**, *334*, 63−70.
(24) Berry, S. M.; Ralle, M.; Low, D. W.; Blackburn, N. J.; Lu, Y. *J. Am. Chem. Soc.* **2003**, *125*, 8760−8768.
(25) Romero, A.; Hoitink, C. W. G.; Nar, H.; Huber, R.; Messerschmidt, A.; Canters, G. W. *J. Mol. Biol.* **1993**, *229*, 1007−1021.
(26) Murphy, L. M.; Strange, R. W.; Karlsson, B. G.; Lundberg, L. G.; Pascher, T.; Reinhammar, B.; Hasnain, S. S. *Jpn. J. Appl. Phys. Part 1* **1993**, *32*, 561−563.
(27) Battistuzzi, G.; Borsari, M.; Canters, G. W.; de Waal, E.; Loschi, L.; Warmerdam, G.; Sola, M. *Biochemistry* **2001**, *40*, 6707−6712.
(28) Xu, F.; Palmer, A. E.; Yaver, D. S.; Berka, R. M.; Gambetta, G. A.; Brown, S. H.; Solomon, E. I. *J. Biol. Chem.* **1999**, *274*, 12 372−12 375.
(29) Pascher, T.; Karlsson, B. G.; Nordling, M.; Malmstrom, B. G.; Vanngard, T. *Eur. J. Biochem.* **1993**, *32*, 289−296.
(30) Palmer, A. E.; Szilagyi, R. K.; Cherry, J. R.; Jones, A.; Xu, F.; Solomon, E. I. *Inorg. Chem.* **2003**, *42*, 4006−4017.
(31) Xu, F.; Shin, W. S.; Brown, S. H.; Wahleithner, J. A.; Sundaram, U. M.; Solomon, E. I. *Biochim. Biophys. Acta* **1996**, *1292*, 303−311.
(32) Ayhan, M.; Xiao, Z. G.; Lavery, M. J.; Hamer, A. M.; Nugent, K. W.; Scrofani, S. D. B.; Guss, M.; Wedd, A. G. *Inorg. Chem.* **1996**, *35*, 5902−5911.
(33) Chen, K. S.; Tilley, G. J.; Sridhar, V.; Prasad, G. S.; Stout, C. D.; Armstrong, F. A.; Burgess, B. K. *J. Biol. Chem.* **1999**, *274*, 36 479−36 487.
(34) Low, D. W.; Hill, M. G. *J. Am. Chem. Soc.* **2000**, *122*, 11 039−11 040.
(35) Libeu, C. A. P.; Kukimoto, M.; Nishiyama, M.; Horinouchi, S.; Adman, E. T. *Biochemistry* **1997**, *36*, 13160−13179.
(36) Machczynski, M. C.; Gray, H. B.; Richards, J. H. *J. Inorg. Biochem.* **2002**, *88*, 375−380.
(37) Hall, J. F.; Kanbi, L. D.; Harvey, I.; Murphy, L. M.; Hasnain, S. S. *Biochemistry* **1998**, *37*, 11 451−11 458.
(38) Li, J.; Nelson, M. R.; Peng, C. Y.; Bashford, D.; Noodleman, L. *J. Phys. Chem. A* **1998**, *102*, 6311−6324.
(39) Wittung-Stafshede, P.; Hill, M. G.; Gomez, E.; Di Bilio, A. J.; Karlsson, B. G.; Leckner, J.; Winkler, J. R.; Gray, H. B.; Malmstrom, B. G. *J. Biol. Inorg. Chem.* **1998**, *3*, 367−370.
(40) Gray, H. B.; Malmstrom, B. G.; Williams, R. J. P. *J. Biol. Inorg. Chem.* **2000**, *5*, 551−559.
(41) Wittung-Stafshede, P.; Gomez, E.; Ohman, A.; Aasa, R.; Villahermosa, R. M.; Leckner, J.; Karlsson, B. G.; Sanders, D.; Fee, J. A.; Winkler, J. R.; Malmstrom, B. G.; Gray, H. B.; Hill, M. G. *Biochim. Biophys. Acta* **1998**, *1388*, 437−443.
(42) Olsson, M. H. M.; Hong, G. Y.; Warshel, A. *J. Am. Chem. Soc.* **2003**, *125*, 5025−5039.
(43) Ryde, U.; Olsson, M. H. M.; Roos, B. O.; De Kerpel, J. O. A.; Pierloot, K. *J. Biol. Inorg. Chem.* **2000**, *5*, 565−574.
(44) Vandekamp, M.; Floris, R.; Hali, F. C.; Canters, G. W. *J. Am. Chem. Soc.* **1990**, *112*, 907−908.
(45) Battistuzzi, G.; Bellei, M.; Borsari, M.; Canters, G. W.; de Waal, E.; Jeuken, L. J. C.; Ranieri, A.; Sola, M. *Biochemistry* **2003**, *42*, 9214−9220.
(46) Battistuzzi, G.; Borsari, M.; Loschi, L.; Menziani, M. C.; De Rienzo, F.; Sola, M. *Biochemistry* **2001**, *40*, 6422−6430.
(47) Botuyan, M. V.; ToyPalmer, A.; Chung, J.; Blake, R. C.; Beroza, P.; Case, D. A.; Dyson, H. J. *J. Mol. Biol.* **1996**, *263*, 752−767.
(48) Lim, C.; Bashford, D.; Karplus, M. *J. Phys. Chem.* **1991**, *95*, 5610−5620.
(49) Bashford, D.; Karplus, M.; Canters, G. W. *J. Mol. Biol.* **1988**, *203*, 507−510.

protein dipoles/Langevin dipoles[55,56] to calculate the difference in the reduction potential of a reference compound outside and inside the protein. The reduction potential of the reference compound can be either taken from experiment or from quantum mechanical calculations, which may also provide the charges of the atoms in the redox active center used in the classical calculations.

We have found only three computational studies[42,47,57] that offer predictions of reduction potentials of T1 copper sites. The structural basis for the difference in reduction potential between poplar plastocyanin and *T. ferrooxidans* rusticyanin have been studied by Botuyan et al.[47] using continuum electrostatics and by Olsson, Hong and Warshel[42] using protein dipole/Langevin dipole and QM/MM techniques. Olsson and Ryde[57] have computed the relative reduction potentials of small models of five T1 copper sites using QM techniques but were not able to reproduce the experimental range of reduction potentials. Thus, a computational rationalization of the wide range of reduction potentials in T1 copper sites has not appeared in the literature.

In this study, we extend our pK_a prediction methodology[58] to the prediction of relative reduction potentials. Quantum mechanical calculations were performed on relatively small structural models derived from X-ray crystal structures of six blue proteins: cucumber stellacyanin,[59,60] *P. aeruginosa* azurin,[61] poplar plastocyanin,[62] *C. cinereus* laccase,[63] *T. ferrooxidans* rusticyanin,[14] and human ceruloplasmin.[64] The relative ordering and range of the reduction potentials of the six T1 copper sites are well reproduced.

The paper is organized as follows. First, we describe the computational methodology employed in this study. Second, we present the results with discussions on the determinants of the relative reduction potentials of T1 copper sites. Third, we compare our results to previous theoretical studies.

II. Computational Methodology

A. Reduction Potential Calculation. For a T1 copper site the free energy change, ΔG, of the electron-transfer reaction

$$\text{protein}\cdot Cu^{2+} + \text{plastocyanin}\cdot Cu^{+} \xrightarrow{\Delta G} \text{protein}\cdot Cu^{+} + \text{plastocyanin}\cdot Cu^{2+} \quad (1)$$

can be related to its reduction potential, $E°$, by the following equation

$$E° = -\frac{\Delta G}{F} + 375\ \text{mV} \quad (2)$$

Here 375 mV is the experimentally measured reduction potential of poplar plastocyanin (vs normal hydrogen electrode) and F is Faraday's constant (0.023 06 kcal·mol^{-1}·mV^{-1}).

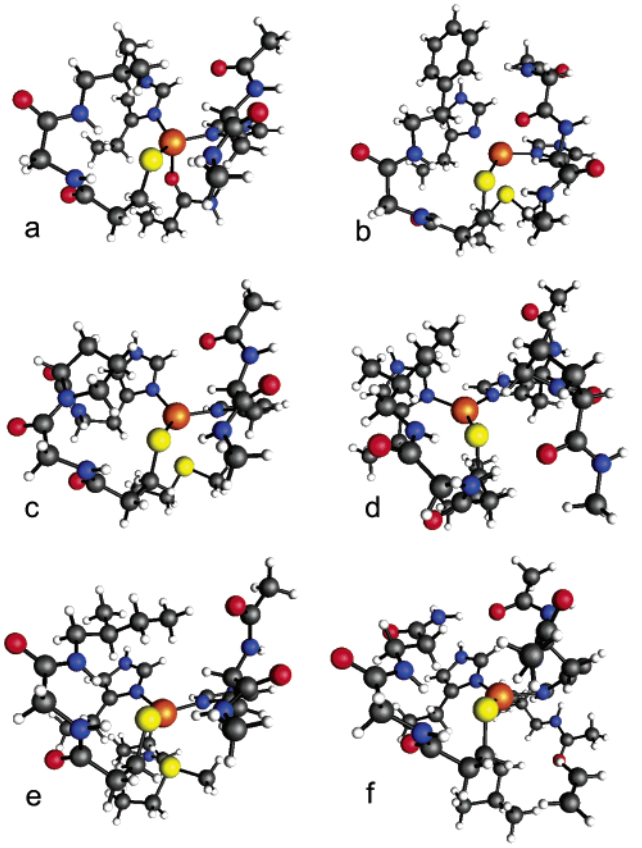

Figure 1. Large models for the type-1 copper sites: (a) cucumber stellacyanin; (b) *P. aeruginosa* azurin; (c) poplar plastocyanin; (d) *C. cinereus* laccase; (e) *T. ferrooxidans* rusticyanin and (f) human ceruloplasmin.

In this study the free energy change, ΔG, is predicted by variously sized model molecules of the proteins in both the gas phase and aqueous solution

$$G_{gas} = E_{ele} \quad (3)$$

$$G_{aq} = E_{ele} + G_{sol} \quad (4)$$

where E_{ele} and G_{sol} are, respectively, the ground-state electronic energy and the solvation energy of a given model.

B. Protein Model Construction. Variously sized structural models for the T1 copper sites were extracted from X-ray crystal structures and edited by manually deleting unwanted atoms and adding new hydrogen atoms to fill the open valencies. The PDB files 1JER,[59] 1AZU,[61] 5PCY,[62] 1HFU,[63] 1RCY[14] and 1KCW[64] were selected for cucumber stellacyanin, *P. aeruginosa* azurin, poplar plastocyanin, *C. cinereus* laccase, *T. ferrooxidans* rusticyanin and human ceruloplasmin, respectively. The hydrogen atoms were added to the PDB files with the WHAT IF web interface.[65]

The large models (LMs, Figure 1) consist of around 100 atoms and include the first layer of the Cu ligands and the hydrophobic groups closest to the Cu. For each large model the positions of the CuSNN atoms and the backbone amide protons (one for *C. cinereus* laccase and two for the other proteins) bound to the S_{Cys} atoms were optimized

(50) Honig, B.; Nicholls, A. *Science* **1995**, *268*, 1144−1149.
(51) Han, W. G.; Lovell, T.; Liu, T. Q.; Noodleman, L. *Inorg. Chem.* **2003**, *42*, 2751−2758.
(52) Torres, R. A.; Lovell, T.; Noodleman, L.; Case, D. A. *J. Am. Chem. Soc.* **2003**, *125*, 1923−1936.
(53) Ullmann, G. M.; Noodleman, L.; Case, D. A. *J. Biol. Inorg. Chem.* **2002**, *7*, 632−639.
(54) Mao, J. J.; Hauser, K.; Gunner, M. R. *Biochemistry* **2003**, *42*, 9829−9840.
(55) Warshel, A.; Papazyan, A.; Muegge, I. *J. Biol. Inorg. Chem.* **1997**, *2*, 143−152.
(56) Stephens, P. J.; Jollie, D. R.; Warshel, A. *Chem. Rev.* **1996**, *96*, 2491−2513.
(57) Olsson, M. H. M.; Ryde, U. *J. Biol. Inorg. Chem.* **1999**, *4*, 654−663.
(58) Li, H.; Robertson, A. D.; Jensen, J. H. *Proteins: Struct. Funct. Bioinform.* **2004**, *55*, 689−704.
(59) Hart, P. J.; Nersissian, A. M.; Herrmann, R. G.; Nalbandyan, R. M.; Valentine, J. S.; Eisenberg, D. *Protein Sci.* **1996**, *5*, 2175−2183.
(60) Nersissian, A. M.; Immoos, C.; Hill, M. G.; Hart, P. J.; Williams, G.; Herrmann, R. G.; Valentine, J. S. *Protein Sci.* **1998**, *7*, 1915−1929.
(61) Adman, E. T.; Jensen, L. H. *Isr. J. Chem.* **1981**, *21*, 8−12.
(62) Guss, J. M.; Harrowell, P. R.; Murata, M.; Norris, V. A.; Freeman, H. C. *J. Mol. Biol.* **1986**, *192*, 361−387.
(63) Ducros, V.; Brzozowski, A. M.; Wilson, K. S.; Ostergaard, P.; Schneider, P.; Svendson, A.; Davies, G. J. *Acta Crystallogr. D* **2001**, *57*, 333−336.
(64) Zaitseva, I.; Zaitsev, V.; Card, G.; Moshkov, K.; Bax, B.; Ralph, A.; Lindley, P. *J. Biol. Inorg. Chem.* **1996**, *1*, 15−23.
(65) Rodriguez, R.; Chinea, G.; Lopez, N.; Pons, T.; Vriend, G. *Bioinformatics* **1998**, *14*, 523−528.

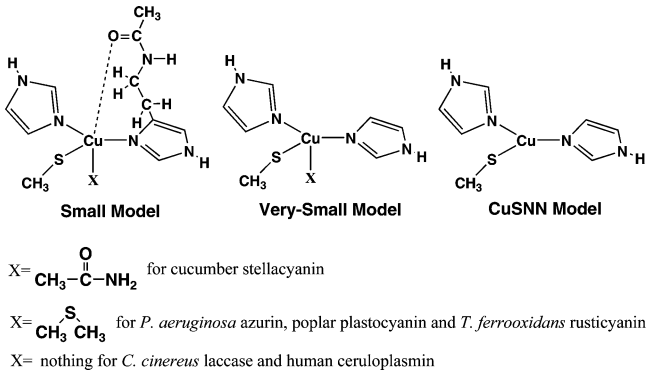

Figure 2. Sketches of the small model (SM), very-small model (VSM) and CuSNN model for the type-1 copper sites.

at the RHF[66]/6-31G*[67,68] and ROHF[69]/6-31G* levels of theory for the Cu^{+} and Cu^{2+} oxidation states, respectively. The positions of the axial S_{Met} atoms for *P. aeruginosa* azurin, poplar plastocyanin and *T. ferrooxidans* rusticyanin, the axial O_{Gln} atom for cucumber stellacyanin, as well as the backbone carbonyl oxygen (Gly45) atom for *P. aeruginosa* azurin, were also optimized.

The small models (SMs, Figure 2) were extracted from the large models. They consist of around 50 atoms, including the Cu ions and the inner sphere ligands. In contrast to the large models, the small models do not have backbone hydrogen bonding to the S_{Cys} atoms and were chosen to be identical to the structural models used by Olsson and Ryde[57] to facilitate comparisons. The very-small models (VSMs, Figure 2) were extracted from the small models by removal of the backbone carbonyl ligands. The CuSNN models (Figure 2) were extracted from the very-small models by removal of the fourth axial ligands and contain only the core: $Cu^{2+/+}(Imidazole)_2(CH_3S^{-})$. For *C. cinereus* laccase and human ceruloplasmin, there is no fourth axial ligand; therefore, the CuSNN models are identical to the very-small models. The geometries of the small, very-small and CuSNN models were not reoptimized.

C. Energy Computation. Gas-phase single point energies (E_{ele}) were computed at the HF/6-31G*,[67,68] B3LYP[70]/6-31G* and MP2[71−73]/6-31G* levels of theory for the model molecules. For the large model's MP2 calculation were performed only for cucumber stellacyanin, poplar plastocyanin and *T. ferrooxidans* rusticyanin due to computational expense. Singlet (RHF[66]) and doublet (ROHF[69]) spin multiplicities were used for Cu^{+} and Cu^{2+}, respectively.

Solvation energies (G_{sol}) of the model molecules in aqueous solution were computed with the integral equation formalism polarizable continuum model (IEF-PCM[74]) at the HF/6-31G* level of theory, with $\epsilon = 78.39$. In the IEF-PCM calculations, the UAHF radii[75] were used for H, C, N, O, S atoms and a radius of 2.40 Å was used for the Cu ions to define the solute cavity, without additional spheres (RET = 100). The 2.40 Å radius for Cu is determined by its bond lengths to the ligation SNNS(or O) atoms, which are between 2.2 Å and 3.7 Å. The GEPOL-GB[76] tessellation procedure was used with 240 initial tesserae per sphere. The ICOMP = 2 method[77] was used for charge renormalization. Only the electrostatic part of the solvation energy was employed for reduction potential calculations.

All quantum mechanical calculations were performed with the GAMESS[78] program. The IEF-PCM/ROHF codes were implemented in GAMESS[78] for this work and will be released in the next version.

Table 1. Comparison of Reduction Potentials (mV) Computed Using Various Structural Models for the Type-1 Copper Sites with Various Methods (see eqs 1−4 and Figures 1, 2)[a]

		method	STEL	PAZU	PLAS	LCAS[b]	RUST	CERL[c]	rmsd5	rmsd4
protein experiment[d]			260	305	375	550	680	≥1000		
gas	SM	HF	−186	332	375	1016	849	1099	*302*	*253*
		B3LYP	27	211	375	872	734	866	*194*	*183*
		MP2	−98	196	375	1025	776	1048	*275*	*250*
	LM	HF	**−172**	**314**	**375**	**676**	**856**	**1170**	***229***	***138***
		B3LYP	22	249	375	432	735	840	*143*	*107*
		MP2	−68		375		790			
		HF (PDB)[e]	−626	420	375	305	369	781	*448*	*233*
Aq.	SM	HF	−232	308	375	635	549	869	*238*	*102*
		B3LYP	−14	201	375	494	438	638	*236*	*226*
		MP2	−139	186	375	646	480	820	*226*	*155*
	LM	HF	−222	355	375	604	627	1028	*220*	*47*
		B3LYP	−29	290	375	360	506	699	*219*	*198*
		MP2	−119		375		561			

[a] STEL, PAZU, PLAS, LCAS, RUST, and CERL represent cucumber stellacyanin, *P. aeruginosa* azurin, poplar plastocyanin, *C. cinereus* laccase, *T. ferrooxidans* rusticyanin, and human ceruloplasmin, respectively. Rmsd5 is the root-mean-square deviation from experiment for STEL, PAZU, LCAS, RUST and CERL (5 in number), whereas rmsd4 is that for PAZU, LCAS, RUST and CERL (4 in number). [b] Cu701 in 1HFU. [c] Cu21 in 1KCW. [d] See discussion section for references. [e] Using the PDB structures without optimization.

III. Results and Discussion

A. Reduction Potential Prediction. The experimental reduction potential values for cucumber stellacyanin (260 mV),[60] *C. cinereus* laccase (550 mV)[63] and *T. ferrooxidans* rusticyanin (680 mV)[5,6] can be readily found in the literature. For *P. aeruginosa* azurin, various values are reported or cited for different pH,[24,29,40] We use the most cited[6,42,57,79] values of 305 mV for pH ≈ 7. For poplar plastocyanin slightly different values (370∼379 mV)[6,40,80] are reported or cited at pH ∼ 7 and we use the value of 375 mV. The redox-inactive T1 copper site in human ceruloplasmin has an unusually high reduction potential (>1000 mV),[13] but the exact value is unknown.

Table 1 presents a comparison of the reduction potentials of six T1 copper sites calculated using the large and small structural models and using Hartree−Fock, density functional theory and second-order perturbation theory, as well as the corresponding experimental values. On the basis of the comparison we seek the simplest possible model that reproduces the ordering and magnitude observed experimentally.

The small models do not yield the correct ordering of the reduction potentials since the value of *C. cinereus* laccase is overestimated. This indicates that the small models are too small to accurately represent the T1 copper sites (see section C for further discussion).

(66) Roothaan, C. C. J. *Rev. Modern Phys.* **1951**, *23*.
(67) Francl, M. M.; Pietro, W. J.; Hehre, W. J.; Binkley, J. S.; Gordon, M. S.; Defrees, D. J.; Pople, J. A. *J. Chem. Phys.* **1982**, *77*, 3654−3665.
(68) Rassolov, V. A.; Pople, J. A.; Ratner, M. A.; Windus, T. L. *J. Chem. Phys.* **1998**, *109*, 1223−1229.
(69) McWeeny, R.; Diercksen, G. *J. Chem. Phys.* **1968**, *49*, 4852−4856.
(70) Hertwig, R. H.; Koch, W. *Chem. Phys. Lett.* **1997**, *268*, 345−351.
(71) Lee, T. J.; Rendell, A. P.; Dyall, K. G.; Jayatilaka, D. *J. Chem. Phys.* **1994**, *100*, 7400−7409.
(72) Lee, T. J.; Jayatilaka, D. *Chem. Phys. Lett.* **1993**, *201*, 1−10.
(73) Pople, J. A.; Binkley, J. S.; Seeger, R. *Int. J. Quantum Chem.* **1976**, *S10*, 1−19.
(74) Cances, E.; Mennucci, B.; Tomasi, J. *J. Chem. Phys.* **1997**, *107*, 3032−3041.
(75) Barone, V.; Cossi, M.; Tomasi, J. *J. Chem. Phys.* **1997**, *107*, 3210−3221.
(76) Pascualahuir, J. L.; Silla, E.; Tunon, I. *J. Comput. Chem.* **1994**, *15*, 1127−1138.
(77) Cossi, M.; Mennucci, B.; Pitarch, J.; Tomasi, J. *J. Comput. Chem.* **1998**, *19*, 833−846.
(78) Schmidt, M. W.; Baldridge, K. K.; Boatz, J. A.; Elbert, S. T.; Gordon, M. S.; Jensen, J. H.; Koseki, S.; Matsunaga, N.; Nguyen, K. A.; Su, S. J.; Windus, T. L.; Dupuis, M.; Montgomery, J. A. *J. Comput. Chem.* **1993**, *14*, 1347−1363.
(79) Olsson, M. H. M.; Ryde, U.; Roos, B. *J. Inorg. Biochem.* **1999**, *74*, 254−254.
(80) McLeod, D. D. N.; Freeman, H. C.; Harvey, I.; Lay, P. A.; Bond, A. M. *Inorg. Chem.* **1996**, *35*, 7156−7165.

Table 2. Coordination Bond Lengths (Å) for the Six Type-1 Copper Sites[a]

		$Cu–S_{Cys}$		$Cu–N_{His}$		$Cu–N_{His}$		$Cu–S_{Met}(O_{Gln})$		$Cu–O_{back}$	
		Cu^+	Cu^{2+}	Cu^+	Cu^{2+}	Cu^+	Cu^{2+}	Cu^+	Cu^{2+}	Cu^+	Cu^{2+}
cucumber	1JER		2.18		1.96		2.04		2.21		3.98
stellacyanin	large M.	2.24	2.24	2.04	1.99	2.01	1.96	2.21	2.14	4.05	4.04
P. *aeruginosa*	1AZU		1.79		2.15		2.42		3.21		2.47
azurin	large M.	2.31	2.28	2.11	2.05	2.15	2.19	3.05	3.06	2.57	2.51
Poplar	5PCY	2.17		2.13		2.39		2.87		4.00	
plastocyanin	large M.	2.28	2.26	2.04	2.02	2.04	1.99	3.24	3.18	3.67	3.73
C. cinereus	1HFU		2.19		2.07		2.03				5.24
laccase[b]	large M.	2.21	2.19	2.03	1.99	2.01	1.99			5.29	5.28
T. ferrooxidans	1RCY		2.26		2.04		1.89		2.89		5.85
rusticyanin	large M.	2.27	2.24	2.07	2.04	2.04	1.97	2.71	2.77	5.94	5.92
Human	1KCW	2.02		2.10		2.05				3.72	
ceruloplasmin[c]	large M.	2.23	2.20	2.08	2.03	2.02	2.00			3.70	3.71

[a] Data are from both PDB crystal structure and partially optimized large models (Figure 1). [b] Cu701 in 1HFU. [c] Cu21 in 1KCW.

For the large models only three MP2 values are available due to computational expense. The performances of HF and B3LYP are roughly the same based on the rmsd from experiment. However, B3LYP does not give the correct ordering when the solvation energy is included, and HF is the only method that predicts a reduction potential of >1000 mV for human ceruloplasmin. Furthermore, the MP2 and HF yield very similar results for both the small and large models. On the basis of these considerations, we choose the gas-phase HF method to study the determinants of reduction potentials in section C.

B. Geometries of the T1 Copper Sites. The copper coordination bond lengths of the crystal structures and the partially optimized large models are listed in Table 2. As mentioned in the methodology section, only the positions of the Cu atom and the atoms "bonded" to Cu (as well as one or two amide protons) are energy minimized. This partial optimization provides the simplest structural model that reproduces the ordering and approximate range of the observed reduction potentials. The optimization is clearly important because reduction potentials evaluated without this modest geometry optimization (Table 1) are not ordered correctly.

Despite the constraints imposed by the fixed atoms, the optimized Cu−ligand bond lengths can change significantly from those of the X-ray structures. Deviations of 0.1∼0.2 Å in Cu−ligand bond lengths are quite common (Table 2), suggesting that the constrained models have some freedom to adjust their geometries. The largest deviation from experiment is 0.5 Å for the $Cu^{2+}–S_{Cys}$ bond length in *P. aeruginosa* azurin, for which the X-ray structure (1AZU) has a low resolution of 2.7 Å. This structure was chosen over higher resolution structures to test the sensitivity of our results to the quality of the X-ray structure. It is gratifying to note that the optimized bond lengths are very similar to those observed in the highest resolution (1.4−1.5 Å) structures of the oxidized and reduced *P. aeruginosa* azurin.[81] The smallest deviations from X-ray structures are for cucumber stellacyanin and *C. cinereus* laccase, for which the X-ray structures have higher resolutions (1.60 and 1.65 Å, respectively). Comparison of the predicted Cu−ligand bond lengths to those obtained from EXAFS studies[20,24,82−85] is equally favorable (data not shown).

The models also have significant freedom to adjust their geometries in response to the change in oxidation state. In cucumber stellacyanin and poplar plastocyanin, the lengths of the bonds to the fourth ligands for the reduced forms are longer by as much as 0.07 Å compared to the oxidized forms. The $Cu–S_{Cys}$ and $Cu–N_{His}$ bond lengths for the reduced forms are systematically longer (by as much as 0.07 Å for *T. ferrooxidans* rusticyanin) than that of the oxidized forms, indicating that the reduced Cu atoms are more out of the plane formed by the S_{Cys}, N_{His1}, and N_{His2} atoms. This is consistent with the trend obtained from the crystal structural data.[40]

The changes tend to be larger for the $Cu–N_{His}$ bonds than the $Cu–S_{Cys}$ bonds when the Cu oxidation states change, presumably due to the differences in the bond strengths.

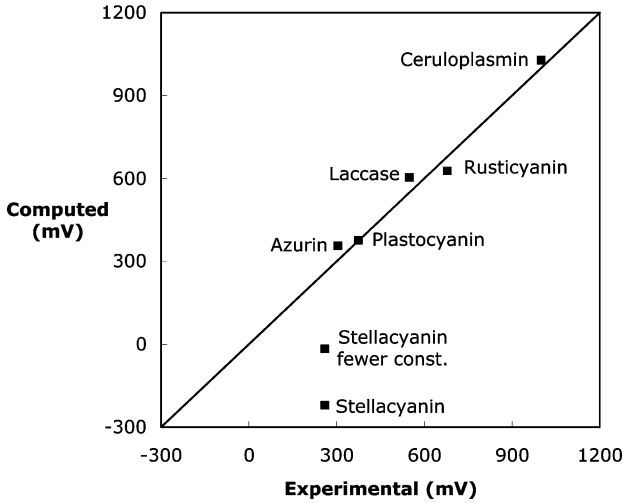

Figure 3. Plot of the experimentally measured reduction potentials vs those predicted using the large models at the RHF/6-31G(d) level of theory in aqueous solution (cf. Table 1). Also shown is the reduction potential of cucumber stellacyanin using fewer structural constraints (see text for details).

C. Determinants of Reduction Potential. Because the relative reduction potentials can be correctly reproduced with the large models (see Figure 3), they must contain the main structural determinants of the relative reduction potential of the six T1 copper sites. These determinants are identified by

(81) Crane, B. R.; Di Bilio, A. J.; Winkler, J. R.; Gray, H. B. *J. Am. Chem. Soc.* **2001**, *123*, 11 623−11 631.
(82) Grossmann, J. G.; Ingledew, W. J.; Harvey, I.; Strange, R. W.; Hasnain, S. S. *Biochemistry* **1995**, *34*, 8406−8414.
(83) DeBeer, S.; Randall, D. W.; Nersissian, A. M.; Valentine, J. S.; Hedman, B.; Hodgson, K. O.; Solomon, E. I. *J. Phys. Chem. B* **2000**, *104*, 10 814−10 819.
(84) Murphy, L. M.; Strange, R. W.; Karlsson, B. G.; Lundberg, L. G.; Pascher, T.; Reinhammar, B.; Hasnain, S. S. *Biochemistry* **1993**, *32*, 1965−1975.
(85) Canters, G. W.; Kolczak, U.; Armstrong, F.; Jeuken, L. J. C.; Camba, R.; Sola, M. *Faraday Discuss.* **2000**, 205−220.

Table 3. Determinants of the Relative Reduction Potentials (mV) for the Type-1 Copper Sites Computed at HF/6-31G* Level of Theory without Solvation[a]

determinants	STEL	PAZU	PLAS	LCAS[b]	RUST	CERL[c]
$\Delta E°$ CuSNN	−49	**+296**	0	−58	**+122**	**+232**
$\Delta E°$ axial ligand	**−571**	+69	0	**+371**	**−106**	**+371**
$\Delta E°$ backbone carbonyl	+59	**−408**	0	**+338**	**+458**	**+121**
$\Delta E°$ H-bonds to S_{Cys}	+14	−18	0	**−340**	+5	+71
$\Delta E°$ total	−547	−61	0	+301	+481	+795
$E°$ LM	−172	314	375	676	856	1170
$E°$ experimental	260	305	375	550	680	≥1000

[a] STEL, PAZU, PLAS, LCAS, RUST, and CERL represent cucumber stellacyanin, *P. aeruginosa* azurin, poplar plastocyanin, *C. cinereus* laccase, *T. ferrooxidans* rusticyanin and human ceruloplasmin, respectively. [b] Cu701 in 1HFU. [c] Cu21 in 1KCW.

recalculating the reduction potentials of successively simpler models. The gas phase energies are used to derive the determinants since solvating the smaller models makes little sense. We emphasize that only the signs of the calculated changes in reduction potentials are expected to be consistent with mutagenesis studies. The magnitudes are expected to be overestimated due to the neglect of compensating intraprotein interactions.

The reduction potential of poplar plastocyanin is analyzed first and used as the reference for the other five proteins. For each protein, the reduction potentials for small, very-small and CuSNN models are obtained by subtracting the differences from the large model value. The determinants of the relative reduction potentials are summarized in Table 3.

Poplar Plastocyanin.

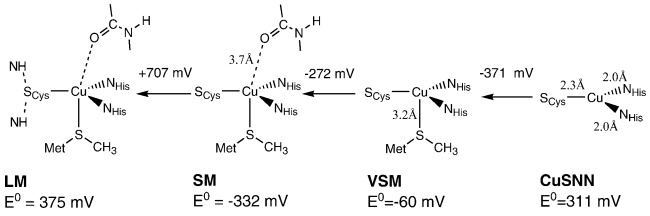

The poplar plastocyanin CuSNN model has a reduction potential of 311 mV.

The axial Met ligand decreases the reduction potential by 371 mV. No mutagenesis study on the axial ligation has been reported for poplar plastocyanin so a direct comparison is not available. Similar studies for cucumber stellacyanin,[20] *P. aeruginosa* azurin,[24] *T. villosa* laccase[28] and *T. ferrooxidans* rusticyanin[22] show that compared to a nonligating Leu or Phe, an axial Met can decrease the reduction potentials by 160, 135, 110, and 131 (pH = 3.2) mV, respectively. Our result for poplar plastocyanin is consistent with these studies.

The backbone carbonyl ligand decreases the reduction potential by 272 mV. The effect of this interaction has not been addressed experimentally.

Adding the backbone carbonyl ligand before the axial Met ligand gives results that are similar to within 11 mV. Similar results are found for all proteins in this study.

The two hydrogen bonds to S_{Cys} increase the reduction potential by 707 mV. Assuming these two hydrogen bonds are of the same strength, then each hydrogen bond increases the reduction potential by ∼350 mV. Experimental mutagenesis of *A. faecalis* pseudoazurin show that the Pro80Ala and Pro80Ile variants have one more backbone hydrogen bond to the copper bound S_{Cys} than the wild type does and show higher reduction potentials (increased by 139 and 180 mV, respectively).[35] Similarly, the Pro94Ala, and Pro94Phe mutants of *P. denitrificans* amicyanin have higher reduction potentials than the wild type (increased by 115 and 150 mV, respectively),[36] presumably due to the creation of a new hydrogen bond to the copper bound S_{Cys}. Our result is consistent with these mutagenesis studies.

Cucumber Stellacyanin.

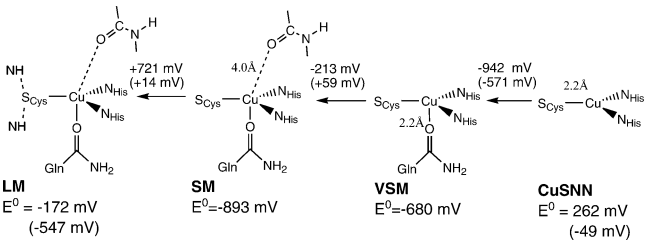

The cucumber stellacyanin CuSNN model has a reduction potential of 262 mV, lower than that of poplar plastocyanin by 49 mV. Obviously, fully optimizing the CuSNN models will give identical reduction potentials for all T1 copper sites. The −49 mV difference is caused by the differences in Cu coordination bond lengths and orientations. For example, the Cu−S_{Cys} bond length is slightly shorter in cucumber stellacyanin (2.24 Å) than that in poplar plastocyanin (2.26∼2.28 Å).

The axial Gln ligand decreases the reduction potential by 942 mV. This change is larger by 571 mV in magnitude than that for poplar plastocyanin where the axial ligand is a Met. This effect is readily explained in terms of the different chemical hardness of the two ligands.[86] The Cu−O_{Gln} bond length in cucumber stellacyanin is 2.2 Å, much shorter than the Cu−S_{Met} bond length of 3.2 Å in poplar plastocyanin. Site-directed mutagenesis studies show that the Gln99Met and Gln99Leu mutants of cucumber stellacyanin exhibit reduction potentials that are 160 and 320 mV higher than the wild type, respectively.[20] Similarly, the Met121Gln[25] and Met121Leu[24] mutants of *P. aeruginosa* azurin have reduction potentials that are 263 mV lower and 135 mV higher than the wild type, respectively. The Met121Gln mutant of *A. denitrificans* azurin has a reduction potential 106 mV lower than the wild type.[27] The Met148Gln and Met148Leu mutants of *T. ferrooxidans* rusticyanin have reduction potentials that are 104 mV lower and 131 mV higher than the wild type, respectively.[22] Our model predicts the correct sign of these changes but overestimates the magnitudes roughly 3-fold.

The backbone carbonyl ligand decreases the reduction potential by 213 mV. This change is smaller by 59 mV in magnitude than that for poplar plastocyanin, presumably due to the longer Cu−O(carbonyl) distance (4.0 vs 3.7 Å).

The two hydrogen bonds to S_{Cys} increase the reduction potential by 721 mV, very similar to that for poplar plastocyanin.

The prime determinant of the lower reduction potential of cucumber stellacyanin compared to poplar plastocyanin thus is the stronger axial ligand interaction in cucumber stellacyanin (Table 3).

(86) Lippard, S. J.; Berg, J. M. *Principles of Bioinorganic Chemistry*; University Science Books: Mill Valley, Calif., 1994.

***P. aeruginosa* Azurin.**

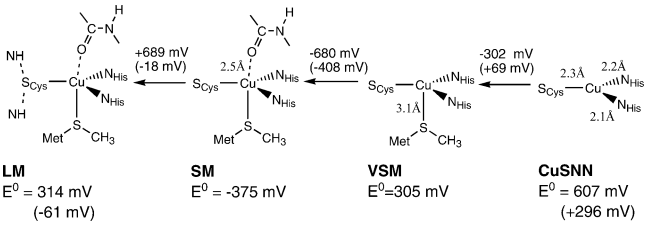

The *P. aeruginosa* azurin CuSNN model has a reduction potential of 607 mV, higher than that of poplar plastocyanin by 296 mV. As discussed above, the difference is caused by the differences in Cu coordination bond lengths and orientations. For example, one $Cu-N_{His}$ bond length is much longer in *P. aeruginosa* azurin (2.15∼2.19 Å) than that in poplar plastocyanin (2.04∼1.99 Å), as shown in Table 2, indicating a weaker Cu−ligand interaction in the former.

The axial Met ligand decreases the reduction potential by 302 mV. This change is smaller in magnitude than that for poplar plastocyanin by 69 mV though the $Cu-S_{Met}$ bond length is slightly shorter in *P. aeruginosa* azurin (Table 2). A site-directed mutagenesis study shows that the Met99Leu mutants of *P. aeruginosa* azurin has a 135 mV higher reduction potential reduction than the wild type.[24] Our model predicts the correct sign of the change with around 2-fold overestimation of the magnitude.

The backbone carbonyl ligand decreases the reduction potential by 680 mV. This change is larger in magnitude than that for poplar plastocyanin by 408 mV, presumably due to the much shorter Cu−O(carbonyl) distance (2.5 Å vs 3.7 Å).

The two hydrogen bonds to S_{Cys} increase the reduction potential by 689 mV, very similar to that for poplar plastocyanin.

The prime determinant of the lower reduction potential of *P. aeruginosa* azurin compared to poplar plastocyanin is the stronger Cu−backbone carbonyl interaction in *P. aeruginosa* azurin. Since the reduction potential of the *P. aeruginosa* azurin CuSNN model is much higher than that of poplar plastocyanin, the overall lowering is relatively small (Table 3). Both effects are due to the protein matrix constraints on the Cu−ligand interactions.

***C. Cinereus* Laccase.**

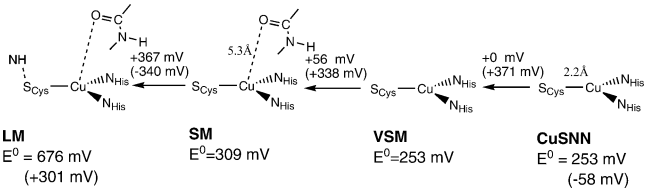

The *C. cinereus* laccase CuSNN model has a reduction potential of 253 mV, lower than that of poplar plastocyanin by 58 mV. As discussed above, the difference is caused by the differences in Cu coordination bond lengths and orientations. For example, the $Cu-S_{Cys}$ bond length is slightly shorter in *C. cinereus* laccase (2.21∼2.19 Å) than that in poplar plastocyanin (2.26∼2.28 Å).

There is neither axial nor backbone carbonyl ligation for *C. cinereus* laccase. Compared to poplar plastocyanin, lack of the fourth ligation increases the reduction potential for *C. cinereus* laccase by 371 mV.

The backbone peptide interaction increases the reduction potential by 56 mV, presumably due to the repulsion between the backbone peptide dipole and Cu^{2+} in *C. cinereus* laccase. In poplar plastocyanin, cucumber stellacyanin, *P. aeruginosa* azurin and human ceruloplasmin (see below) there are attractions between the backbone peptide dipole and Cu^{2+}. Compared to poplar plastocyanin, lack of the fifth ligand increases the reduction potential for *C. cinereus* laccase by 338 mV.

The hydrogen bond to S_{Cys} increases the reduction potential by 367 mV, roughly the half of the values for poplar plastocyanin, cucumber stellacyanin, *P. aeruginosa* azurin and human ceruloplasmin (see below), which have two such hydrogen bonds. Compared to poplar plastocyanin, one less hydrogen bond decreases the reduction potential for *C. cinereus* laccase by 340 mV.

The prime determinant of the higher reduction potential of *C. cinereus* laccase compared to poplar plastocyanin is the absence of axial and backbone carbonyl ligand interaction. Because *C. cinereus* laccase has one less hydrogen bond to the S_{Cys}, the overall increase in reduction potential is lowered somewhat (Table 3).

***T. Ferrooxidans* Rusticyanin.**

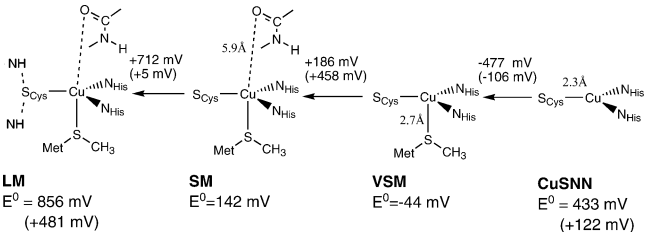

The *T. ferrooxidans* rusticyanin CuSNN model has a reduction potential of 433 mV, higher than that of poplar plastocyanin by 122 mV. The difference is very likely caused by the differences in the orientations of the Cu ligands since the bond lengths are very similar.

The axial Met ligand decreases the reduction potential by 477 mV. This change is larger in magnitude than that for poplar plastocyanin by 106 mV, presumably due to the shorter $Cu-S_{Met}$ bond length (2.7 Å vs 3.2 Å). A site-directed mutagenesis study shows that the Met148Leu mutant of *T. ferrooxidans* rusticyanin has a 131 mV higher (pH = 3.2) reduction potential than the wild type.[22] Our model predicts the correct sign of the change with around 3-fold overestimation of the magnitude.

There is no backbone carbonyl ligation for *T. ferrooxidans* rusticyanin. Similar to *C. cinereus* laccase, the backbone peptide interaction increases the reduction potential by 186 mV. As discussed above, this is presumably due to the repulsion between the backbone peptide dipole and Cu^{2+} in *T. ferrooxidans* rusticyanin and *C. cinereus* laccase. Compared to poplar plastocyanin, lack of the fifth ligation increases the reduction potential of *T. ferrooxidans* rusticyanin by 458 mV.

The two hydrogen bonds to S_{Cys} increase the reduction potential by 712 mV, similar to that in poplar plastocyanin.

The prime determinant for the higher reduction potential of *T. ferrooxidans* rusticyanin compared to poplar plastocyanin is the absence of backbone carbonyl ligand interaction. The intrinsically higher reduction potential of the CuSNN model is

largely canceled by the stronger axial Met ligand interaction (Table 3).

Human Ceruloplasmin.

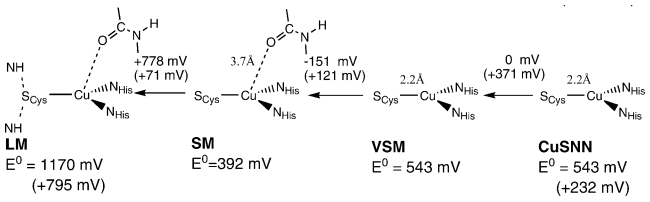

The human ceruloplasmin CuSNN model has a reduction potential of 543 mV, higher than for poplar plastocyanin by 232 mV. The difference is probably caused by the differences in the orientations of the Cu ligands since the bond lengths are very similar. For example, the angle between one histidine plane and its Cu−N_{His} bond is ∼28°, unusually large. Such angles are usually <5° in T1 copper sites.

There is no axial ligand for human ceruloplasmin. Compared to poplar plastocyanin, lack of the fourth ligation increases the reduction potential for human ceruloplasmin by 371 mV.

The backbone carbonyl ligand decreases the reduction potential by 151 mV, smaller in magnitude than that for poplar plastocyanin by 121 mV. Since the Cu−O(carbonyl) distances are the same (3.7 Å) for human ceruloplasmin and poplar plastocyanin, the difference is probably caused by the different interaction between the backbone peptide dipole and Cu^{2+}.

The two hydrogen bonds to S_{Cys} and the one to the backbone carbonyl oxygen increase the reduction potential by 778 mV, similar to that for poplar plastocyanin.

The determinants of the higher reduction potential of human ceruloplasmin compared to poplar plastocyanin thus are (1) the absence of axial ligand, (2) higher intrinsic CuSNN reduction potential, and (3) weaker backbone carbonyl ligand interaction, as shown in Table 3.

D. Discussion. The five general determinants of reduction potential listed in the Introduction section are discussed below in light of our findings:

(1) Desolvation of the T1 copper sites. Our results show that this factor does not appear to be the major determinant of the *relative* reduction potentials, though in general it may raise the T1 site reduction potential compared to that of the aqueous Cu^{2+}/Cu^{+} pair.[14−18] The very high reduction potential of *T. ferrooxidans* rusticyanin has been attributed to the unusually high hydrophobicity[14,15,18,19] compared to those of other blue copper proteins. However, according to our model, the higher value of *T. ferrooxidans* rusticyanin is primarily due to a weaker Cu−carbonyl interaction than that for cucumber stellacyanin, *P. aeruginosa* azurin and poplar plastocyanin.

(2) Metal−ligand interaction. Our results show that axial Met and Gln ligands can decrease the T1 copper reduction potential, consistent with site-directed mutagenesis studies of T1 copper sites.[20−29] The difference in axial ligand is responsible for the lower reduction potential of cucumber stellacyanin relative to poplar plastocyanin. Furthermore, the lack of axial ligand is an important part of the reason for the higher reduction potential of *C. cinereus* laccase and human ceruloplasmin. Our models also show that the backbone carbonyl ligation can decrease the reduction potentials. The stronger Cu−O(carbonyl) interaction is the main reason for the lower reduction potential of *P. aeruginosa* azurin relative to poplar plastocyanin, whereas a weaker interaction in *C. cinereus* laccase and *T. ferrooxidans* rusticyanin contributes significantly to their higher reduction potentials. Unfortunately, no experimental backbone engineering study is available for comparison. However, the importance of the Cu−O(carbonyl) interaction in modulating the reduction potentials of T1 sites has previously been postulated by Malmström and co-workers.[39,87]

(3) Hydrogen bonding to the copper bound S_{Cys}. Our results show that backbone amide-S_{Cys} hydrogen bonding increases T1 copper reduction potential, consistent with mutagenesis studies involving proline residues that create a new hydrogen bond on the copper bound S_{Cys} atoms.[35,36] However, because all of the proteins studied in this work except for *C. cinereus* laccase have two such hydrogen bonds, their relative reduction potentials are not determined by this factor. In *C. cinereus* laccase, the reduction potential increase due to the lack of axial ligation [including that of the fifth O(carbonyl)] is attenuated by the lack of one hydrogen bond.

(4) Protein constraint. Our results show that this factor is one of the major determinants of the relative reduction potentials, though experimental[85,88] and theoretical[43,89,90] studies show that in general the trigonally distorted tetrahedral coordination geometries of the T1 Cu^{2+} sites are not due to protein constraint. A recent theoretical calculation,[20] however, shows that protein constraint on the cucumber stellacyanin T1 copper center can cause ∼7 kcal/mol energy difference, which would correspond to a ∼300 mV change in reduction potential. In our models, the ligands are fixed in position in order to mimic the forces imposed by the protein matrix. According to our models, relatively small changes in the CuSNN coordination bond lengths and orientations can cause relatively large changes (∼350 mV) in reduction potential. The structural differences in the CuSNN models are ultimately due to the protein fold or constraint. Furthermore, the position of the backbone carbonyl ligand, which has a significant effect on the reduction potential, is also dictated by the protein fold.

(5) Intraprotein electrostatic interaction. Our results show that only the amide dipoles directly bonded to S_{Cys} and the backbone peptide dipole closest to Cu appear to be major determinants of the relative reduction potentials. In general, site-directed mutations involving charged groups tend to cause at most ∼120 mV change in the reduction potential, including the charge mutations of the axial ligands.[21,22,26,27,29,37,44−46] For example, Met121Glu[21] and Met121Asp[26] *P. aeruginosa* azurins,[26] Met148Glu,[22] Met148Lys,[22] and Ser86Asp[37] *T. ferrooxidans* rusticyanins show ∼100, 20, 116, 117, and 44 mV decreases in reduction potential compared to the wild types. In the wild-type copper proteins charged side chains tend to be >9 Å from the T1 sites and tend to be on the protein surface, where the charge is largely screened by solvent. Thus neither short- nor long-range charge−charge interactions appear to be a major factor in regulating the reduction potential. However, though

(87) Malmstrom, B. G.; Leckner, J. *Curr. Opin. Chem. Biol.* **1998**, *2*, 286−292.
(88) Wijma, H. J.; Boulanger, M. J.; Molon, A.; Fittipaldi, M.; Huber, M.; Murphy, M. E. P.; Verbeet, M. P.; Canters, G. W. *Biochemistry* **2003**, *42*, 4075−4083.
(89) Ryde, U.; Olsson, M. H. M.; Pierloot, K.; Roos, B. O. *J. Mol. Biol.* **1996**, *261*, 586−596.
(90) Olsson, M. H. M.; Ryde, U.; Roos, B. O.; Pierloot, K. *J. Biol. Inorg. Chem.* **1998**, *3*, 109−125.

Table 4. Computed Reduction Potentials (mV) for the Six Type-1 Copper Sites and Comparison to Previous Calculations

	QM, this work		QM, Olsson et al.		Botuyan et al.[c]		
	LM vacuum	SM in aq.	SM[a] in aq.	protein[b] in aq.	NMR struct.	X-ray struct.	exp[d]
cucumber stellacyanin	−172	−14	340				260
P. aeruginosa azurin	314	201	327				305
Poplar plastocyanin	375	375	375	375	375	375	375
C. cinereus laccase[e]	676	494					550
T. ferrooxidans rusticyanin	856	439	470	684	603	764	680
human ceruloplasmin[f]	1170	638	440				>1000

[a] Ref 57. [b] Ref 42. [c] Ref 47. [d] See discussion section for references. [e] Cu701 in 1HFU. [f] Cu21 in 1KCW.

the charge−charge interactions have small effects on reduction potential, dipole interactions from the protein peptide backbone and the polar side chain groups are more important (∼300 mV) according to some theoretical studies.[42,47]

E. Comparison to Previous Calculations. Three computational studies[42,47,57] that predict reduction potentials of T1 copper sites have appeared in the literature. A comparison of our predictions with those in previous works is presented in Table 4.

QM Models. Olsson and Ryde[57] have published predictions of the relative reduction potentials of five of the six proteins considered in this study (*C. cinereus* laccase was not included). They used B3LYP and PCM to calculate E_{ele} and G_{sol} [see eq 2] with chemical models that are identical to the small models considered here. The main difference between their and our studies is that they performed complete geometry optimizations except that the distances between the Cu atom and the axial ligands (including the backbone carbonyl) were constrained to X-ray structural values of the oxidized and reduced forms.

Olsson and Ryde's results (Table 4) can be directly compared to our B3LYP aqueous solution results using the small models. Compared to our SM results the reduction potentials of cucumber stellacyanin and human ceruloplasmin are significantly over- and underestimated, respectively, by Olsson and Ryde's approach. On the basis of our analysis (Table 3) the ∼200 mV difference observed for human ceruloplasmin is probably due to relaxation of the protein-induced distortion of the CuSNN core, a constraint that we predict to be an important determinant of its high reduction potential. Furthermore, the data in Table 1 indicate that B3LYP tend to underestimate the reduction potential relative to RHF and MP2, and that a larger model for human ceruloplasmin including the Leu residue at the axial position is needed if the PCM solvation energy is included.

The cause of the difference in the reduction potential of cucumber stellacyanin predicted by us and by Olsson and Ryde using the small models is less clear. The main structural difference is the $Cu-O_{Gln}$ distances, which Olsson and Ryde constrained to be 2.69 Å and 2.25 Å for Cu^+ and Cu^{2+}, respectively. These values were taken from the X-ray structures of the Met121Gln mutant[25] of *P. aeruginosa* azurin because an X-ray structure of the reduced stellacyanin was not available at the time of the study. The value of 2.69 Å is much longer than our predicted value of 2.21 Å for the Cu^+ form (our predicted $Cu^{2+}-O_{Gln}$ distance is 2.14 Å). It is thus possible that the overestimation of the relative reduction potential predicted by Olsson and Ryde's model is primarily due to the use of a Cu^+-O_{Gln} bond length that is too long. Conversely, our model underestimates the reduction potential of cucumber stellacyanin relative to poplar plastocyanin, possibly due to a Cu^+-O_{Gln} bond length that is too short as a result of the constraints imposed. Removal of the constraints on the two H^γ atoms, the C^δ atom, the N^ϵ atom and the two H^ϵ atoms of the cucumber stellacyanin Gln99 side chain and reoptimization of the small model lead to $Cu-O_{Gln}$ distances of 3.80 Å and 2.22 Å, respectively, for the Cu^+ and Cu^{2+} forms, and a reduction potential of 19 mV. This is consistent with the experimental observation that the reduced form has a longer $Cu-O_{Gln}$ distance than the oxidized form in the Met121Gln mutant[25] of *P. aeruginosa* azurin, which is considered as a good model for stellacyanin. However, no experimental data of cucumber stellacyanin is available for a direct comparison. Our model suggests that upon reduction the $Cu-O_{Gln}$ interaction becomes very weak and the O_{Gln} tends to leave the Cu^+.

In short, the differences between Olsson and Ryde's results and ours for the small models are understood. On the basis of our analysis, larger models including the nonligating groups at the axial positions for *C. cinereus* laccase and human ceruloplasmin must be used if PCM solvation energy is included. Furthermore, larger models including hydrogen bonding to the S_{Cys} atom are in general necessary for accurate predictions of the relative reduction potentials of T1 copper sites.

Electrostatic Models. Botuyan et al.[47] predicted the relative reduction potentials for poplar plastocyanin and *T. ferrooxidans* rusticyanin using a continuum electrostatic model. The reduction potential differences obtained by NMR structures and X-ray structures are 228 mV and 389 mV, respectively (Table 4). Using protein dipole/Langevin dipole and QM/MM frozen density functional free energy simulation techniques, Olsson, Hong and Warshel[42] predicted similar values for this pair (∼300 mV, Table 4). Both studies suggest that the reduction potential differences between poplar plastocyanin and *T. ferrooxidans* rusticyanin is caused by many small protein dipole interactions with the Cu ions, while our results suggest that the prime determinant is a single backbone carbonyl group. It is not clear which interpretation is correct. However, our analysis clearly leads to the hypothesis that significantly elongating the Cu−O(carbonyl) distance in poplar plastocyanin by mutation or backbone engineering should increase the reduction potential to a value near that of *T. ferrooxidans* rusticyanin.

Acknowledgment. This work was supported by a grant from the National Science Foundation (MCB 0209941). H.L. gratefully acknowledges a predoctoral fellowship from the Center for Biocatalysis and Bioprocessing at the University of Iowa. The calculations were performed on IBM RS/6000 workstations and an eight-node QuantumStation obtained through NSF grants CHE 9974502 and MCB 0209941, respectively, and on computers at the Advanced Biomedical Computing Center (ABCC), SAIC-Frederick, National Cancer Institute at Frederick. H.L. thanks the ABCC for their warm hospitality during the summer of 2003. This project has been supported in part with Federal funds from the National Cancer Institute, National Institutes of Health, under Contract No. N01-CO-12400. We thank Profes-

sors Harry Gray, S. Ramaswamy, and Jason Telford for valuable suggestions on the manuscript. The content of this publication does not necessarily reflect the views or policies of the Department of Health and Human Services, nor does the mention of trade names, commercial products or organization imply endorsement by the U.S. Government

JA049345Y